PHYSICAL REVIEW A **80**, 023407 (2009)

Coherent control of vibrational population transfer in the Li_2 molecule with femtosecond laser pulses in the presence of manifolds of rotational levels

Chitrakshya Sarkar, S. S. Bhattacharyya, and Samir Saha
Department of Materials Science, Atomic and Molecular Physics Section, Indian Association for the Cultivation of Science, Jadavpur, Kolkata 700032, India

(Received 30 March 2009; revised manuscript received 25 May 2009; published 11 August 2009)

We have theoretically investigated the vibrational population transfer in the presence of manifolds of rotational levels in a model 15-level Li_2 molecular system by stimulated Raman adiabatic passage with intense unchirped femtosecond laser pulses. We have considered five rotational levels $J_g=0,2,\ldots,8$ associated with the initial vibrational level $v_g=0$ of the ground electronic state $X\,^1\Sigma_g^+$, five rotational levels $J_i=1,3,\ldots,9$ associated with the vibrational level $v_i=1$ of the intermediate excited electronic state $A\,^1\Sigma_u^+$, and five rotational levels $J_f=0,2,\ldots,8$ associated with the final target vibrational levels $v_f=1,2$ of the $X\,^1\Sigma_g^+$ state of the Li_2 alkali dimer. The pump and Stokes laser pulses are taken to have the same temporal (Gaussian) shapes, pulse widths, and linear parallel polarizations. The laser wavelengths are in the (visible) range of 700–740 nm. The (peak) intensities of the pulses are of the order of $1\times10^{12}-2.5\times10^{13}$ W/cm^2 and the pulse widths are of the order of 20–50 fs. We have solved the 15 coupled time-dependent Schrödinger equations to study the population transfer to the target-excited vibrational levels. We have observed that, even with "mushrooming" of closely spaced rotational levels, efficient and selective population transfer to excited vibrational levels in Li_2 alkali dimer can be achieved for counterintuitive pulse sequence by controlling the pump and Stokes laser parameters. We have endeavored to explain the results within the framework of adiabatic picture.

DOI: 10.1103/PhysRevA.80.023407 PACS number(s): 33.80.Be, 42.50.Hz, 42.65.Dr

I. INTRODUCTION

In recent years, the preparation of atoms and molecules in well-defined quantum states has become important for the study of collision dynamics, laser controlled chemical reactions, atom optics, quantum information, and spectroscopy. The development of efficient schemes for selective population transfer to excited levels has been a challenging task for many workers in this field. The stimulated Raman adiabatic passage (STIRAP) [1,2] is now a well-established technique for efficient population transfer to a particular excited atomic or molecular level. The three conditions which are prerequisite for STIRAP in a three-level Λ system are (i) two-photon Raman resonance between the initially populated level and the final (target) level, (ii) the pump and Stokes laser pulses are applied in the counterintuitive sequence where the Stokes pulse coupling the excited intermediate level to the final (target) level precedes the pump pulse coupling the initial (ground) level to the excited intermediate level with partial overlap between the pulses, and (iii) adiabatic time evolution of the system.

The first experimental work on STIRAP was performed by Gaubatz *et al.* [3,4] for Na_2 alkali dimers for near- and on-resonance excitations. They investigated in detail the population transfer for intuitive, counterintuitive, and simultaneous pulsed lasers with intermediate level detunings $\Delta<0$, $\Delta=0$, and $\Delta>0$. They observed complete population transfer for counterintuitive pulse sequence when the pump and Stokes frequencies were tuned to resonance in spite of the fact that the excited intermediate level has a shorter lifetime than the laser-pulse duration. These experimental results on STIRAP were verified by Band and Julienne [5] who have done numerical calculations for Na_2 molecule using the density-matrix technique with Gaussian pulses. A theoretical description for a multilevel system where population transfer was achieved to the desired level was accomplished by solving the coupled time-dependent Schrödinger equations (TDSE) both analytically and numerically by Shore *et al.* [6]. Coulston and Bergmann [7] studied analytically the STIRAP process for model multilevel systems where pump and Stokes lasers coupled levels close to the intermediate and final levels outside the three-level Λ system. They found high population transfer efficiency to the final level with certain criteria for the controllable parameters. They compared their analytical results with numerical computations using the density-matrix method. Vitanov and Stenholm [8] analytically studied the population transfer problem in a model three-level Λ system for different pulse shapes. Special emphasis was given to study the effect of pulse order on population transfer efficiency. They also examined the STIRAP process for a three-level system considering the effect of irreversible dissipation from the excited intermediate state on population transfer by solving the coupled TDSE. A generalized study of STIRAP in which the single intermediate state is replaced by N intermediate states was also studied by Vitanov and Stenholm [9], where each of these states is connected to the initial state with a coupling proportional to the pump pulse and to the final state with a coupling proportional to the Stokes pulse, thus forming a parallel multi-Λ system. They derived the conditions for existence of a more general adiabatic-transfer state that includes transient contributions from the intermediate states but still transfer of population was achieved from the initial to the final states in the adiabatic limit. They discussed various numerical examples for success and failures of the multi-STIRAP process. Ghosh *et al.* [10] theoretically investigated the effect of nonadiabatic (NA) interaction on the population transfer in a four-level H_2 molecular system by STIRAP technique where two excited intermediate resonant levels are coupled with each other by NA interaction, using the density-matrix method with Gaussian pump and Stokes laser pulses. They also theoretically studied the effect of polarization on population transfer in a six-level H_2 molecule [11] by STIRAP process using the density-matrix technique with Gaussian pulses where they have shown in detail the dependence of population transfer on time delay between the two pulses for the case of on-resonance excitations considering linear parallel as well as same-sense circular polarizations of the two fields. Légaré *et al.* [12] studied the population transfer by Raman chirped nonadiabatic passage (RCNAP) in a model three-level as well as in a multilevel H_2 system comprising of 17 rotational levels of the H_2 molecule by solving the coupled TDSE. The 17-level H_2 system consisted of six rotational levels $J=0,2,\ldots,10$ associated with the initial vibrational level $v=0$ of the ground electronic state $X\,{}^1\Sigma_g^+$, five rotational levels $J=1,3,\ldots,9$ associated with the intermediate vibrational level $v=5$ of the excited electronic state $B\,{}^1\Sigma_u^+$, and six rotational levels $J=0,2,\ldots,10$ associated with the final excited vibrational level $v=12$ of the $X\,{}^1\Sigma_g^+$ state.

Recently, Band *et al.* [13] performed numerical calculations to obtain complete selective population transfer in Na_2 alkali dimers using chirped simultaneous laser pulses of picosecond order, shorter than the molecular rotation time. They used a wave-packet method for state selective population transfer to a rovibrational level of an excited electronic state with "mushrooming" of closely spaced rotational levels. They studied a model ten-level Na_2 molecular system with $J=0,2,4,6$ of $v=0$ in the initial ground $X\,{}^1\Sigma_g^+$ manifold, $J=1,3,5$ of $v=0$ in the first-excited $A\,{}^1\Sigma_u^+$ manifold, and $J=2,4,6$ of $v=0$ of the second-excited $2\,{}^1\Pi_g$ manifold of the molecule.

In the present paper, we have investigated the vibrational population transfer in the presence of manifolds of rotational levels in a model 15-level Li_2 molecular system (Fig. 1) by STIRAP process with unchirped femtosecond (broad band) laser pulses. In Li_2 alkali dimer, owing to its very small value of the rotational constant B_e (0.6726 cm^{-1}) [14] compared to that (60.85 cm^{-1}) of H_2, the rotational levels are very closely spaced (few cm^{-1}) and in fact there is mushrooming of rotational levels in molecules such as Li_2. The effect of this mushrooming of rotational levels on vibrational population transfer in Li_2 by STIRAP becomes important for femtosecond pulsed lasers where we also have to incorporate the counter-rotating wave terms [15] beyond the rotating wave approximation (RWA) [1,2] in the Hamiltonian. The laser-pulse durations are taken in the femtosecond range because they are appropriate or adequate in the transform-limited bandwidth for coverage of the clusters of rotational levels $J=0,2,\ldots,8$ for the initial ground ($v_g=0$) and final target ($v_f=1,2$) vibrational levels of the $X\,{}^1\Sigma_g^+$ electronic state and $J=1,3,\ldots,9$ of the intermediate excited $A\,{}^1\Sigma_u^+$ electronic state of the Li_2 alkali molecule.

In Sec. II, we present the formulation of STIRAP process for the 15-level Li_2 system using the coupled TDSE with Gaussian pulses. In Sec. III, we briefly discuss the ways the calculations have been performed and the laser parameters used in the calculations. In Sec. IV, we illustrate and discuss the results. Finally, in Sec. V, we give a brief conclusion.

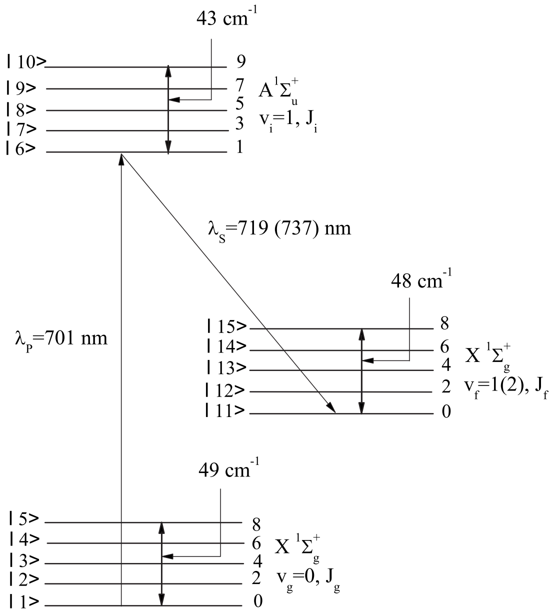

FIG. 1. Schematic energy-level diagram showing the relevant 15 rovibrational levels of the ground $X\,{}^1\Sigma_g^+$ and excited $A\,{}^1\Sigma_u^+$ electronic states of Li_2 molecule for (1+1)-photon stimulated Raman process with pump and Stokes laser pulses of wavelengths λ_P and λ_S.

II. FORMULATION

This section describes the formulation of population transfer process in a model 15-level Li_2 alkali dimer by (1+1)-photon STIRAP. The 15-level system under consideration is shown schematically in Fig. 1 where all the relevant state levels are indicated. We have solved the 15 coupled TDSE for this model system to get the populations of various levels of the system interacting with the pump and Stokes laser pulses of femtosecond (broad band) pulse widths.

The N-coupled time-dependent Schrödinger equations for the system can be written as (in a.u.)

$$i\frac{d}{dt}\boldsymbol{C}(t)=\boldsymbol{H}(t)\boldsymbol{C}(t), \tag{1}$$

where $\boldsymbol{C}(t)=[C_1(t),C_2(t),\ldots,C_{N-1}(t),C_N(t)]^T$ give the time-dependent probability amplitudes of the level populations and $\boldsymbol{H}(t)=\boldsymbol{H}_0+\boldsymbol{H}_I(t)$ is the total Hamiltonian, where $\boldsymbol{H}_0$ is the time-independent unperturbed Hamiltonian of the molecule plus the laser fields and $\boldsymbol{H}_I(t)$ is the interaction Hamiltonian between the molecule and the laser fields. $\boldsymbol{H}_I(t)$ in the electric field gauge (with dipole approximation) is expressed as

$$\boldsymbol{H}_I(t)=-\boldsymbol{E}_P(t)\cdot\boldsymbol{d}-\boldsymbol{E}_S(t)\cdot\boldsymbol{d}, \tag{2}$$

where $\boldsymbol{E}_P(t)$ and $\boldsymbol{E}_S(t)$ are the electric fields of the pump and Stokes pulses, respectively. $\boldsymbol{d}$ is the electric transition dipole operator. The classical forms of $\boldsymbol{E}_P(t)$ and $\boldsymbol{E}_S(t)$ for linearly polarized light are given by

$$\boldsymbol{E}_P(t)=\left(\tfrac{1}{2}\right)f_P(t)(I_P^0)^{1/2}\hat{\varepsilon}_P(e^{i\omega_P t}+e^{-i\omega_P t}),$$

and

$$\boldsymbol{E}_S(t) = (\tfrac{1}{2}) f_S(t)(I_S^0)^{1/2}\hat{\varepsilon}_S(e^{i\omega_S t}+e^{-i\omega_S t}), \tag{3}$$

where ω_P and ω_S are the frequencies of the pump and Stokes lasers, $\hat{\varepsilon}_P$ and $\hat{\varepsilon}_S$ represent the unit polarization vectors of the incident linearly polarized pump and Stokes fields, I_P^0 and I_S^0 are the peak intensities of the pump and Stokes laser pulses, while $f_P(t)$ and $f_S(t)$ express the time variations of the laser field amplitudes. The functional forms of $f_P(t)$ and $f_S(t)$ are taken to be Gaussian [10]

$$f_P(t) = \exp[-(t-t_p)^2/(2\tau_P^2)],$$

and

$$f_S(t) = \exp[-\{t-(t_p+\Delta t)\}^2/(2\tau_S^2)], \tag{4}$$

where τ_P and τ_S are the pulse widths, Δt is the time delay between the pulses, and t_p is the pulse scaling time. For $\Delta t > 0$, the pump pulse precedes the Stokes pulse and specifies intuitive pulse order whereas $\Delta t < 0$ corresponds to the counterintuitive pulse sequence where the Stokes pulse precedes the pump pulse.

The 15 coupled TDSE, without RWA, that is, with inclusion of the counter-rotating wave terms [15], reduce to, after some (phase) transformations (Fig. 1),

$$i\frac{d\tilde{C}_1(t)}{dt} = \Omega_{1,6}^P(t)(1+e^{-i2\omega_P t})\tilde{C}_6(t),$$

$$\begin{aligned} i\frac{d\tilde{C}_2}{dt} &= \Delta_{2,1}\tilde{C}_2(t) + \Omega_{2,6}^P(t)(1+e^{-i2\omega_P t})\tilde{C}_6(t) \\ &\quad + \Omega_{2,7}^P(t)(1+e^{-i2\omega_P t})\tilde{C}_7(t), \end{aligned}$$

$$\vdots$$

$$\begin{aligned} i\frac{d\tilde{C}_6(t)}{dt} &= \Delta_{6,1}^P\tilde{C}_6(t) + \Omega_{6,1}^P(t)(1+e^{i2\omega_P t})\tilde{C}_1(t) \\ &\quad + \Omega_{6,2}^P(t)(1+e^{i2\omega_P t})\tilde{C}_2(t) + \Omega_{6,11}^S(t)(1+e^{i2\omega_S t}) \\ &\quad \times\tilde{C}_{11}(t) + \Omega_{6,12}^S(t)(1+e^{i2\omega_S t})\tilde{C}_{12}(t), \end{aligned}$$

$$\begin{aligned} i\frac{d\tilde{C}_7(t)}{dt} &= \Delta_{7,1}^P\tilde{C}_7(t) + \Omega_{7,2}^P(t)(1+e^{i2\omega_P t})\tilde{C}_2(t) \\ &\quad + \Omega_{7,3}^P(t)(1+e^{i2\omega_P t})\tilde{C}_3(t) + \Omega_{7,12}^S(t) \\ &\quad \times(1+e^{i2\omega_S t})\tilde{C}_{12}(t) + \Omega_{7,13}^S(t)(1+e^{i2\omega_S t})\tilde{C}_{13}(t), \end{aligned}$$

$$\vdots$$

$$\begin{aligned} i\frac{d\tilde{C}_{14}(t)}{dt} &= \Delta_{14,1}^{P+S}\tilde{C}_{14}(t) + \Omega_{14,8}^S(t)(1+e^{-i2\omega_S t})\tilde{C}_8(t) \\ &\quad + \Omega_{14,9}^S(t)(1+e^{-i2\omega_S t})\tilde{C}_9(t), \end{aligned}$$

$$\begin{aligned} i\frac{d\tilde{C}_{15}(t)}{dt} &= \Delta_{15,1}^{P+S}\tilde{C}_{15}(t) + \Omega_{15,9}^S(t)(1+e^{-i2\omega_S t})\tilde{C}_9(t) + \Omega_{15,10}^S(t) \\ &\quad \times(1+e^{-i2\omega_S t})\tilde{C}_{10}(t), \end{aligned} \tag{5}$$

where $\Delta_{2,1},\Delta_{6,1}^P,\ldots,\Delta_{15,1}^{P+S}$ are detunings of the different vibrational-rotational levels with respect to the initial rovibrational level $v_g=0$, $J_g=0$ (marked as 1) of the $X\,{}^1\Sigma_g^+$ state (Fig. 1). These detunings are given by

$$\Delta_{2,1} = \omega_2 - \omega_1,$$

$$\vdots$$

$$\Delta_{6,1}^P = \omega_6 - \omega_1 - \omega_P,$$

$$\vdots$$

$$\Delta_{15,1}^{P+S} = \omega_{15} + \omega_S - \omega_1 - \omega_P, \tag{6}$$

where ω_i signifies the energy of the $|i\rangle$ level. The expression for the one-photon Rabi frequency coupling the levels $|i\rangle$ and $|j\rangle$ of different electronic states is given by

$$\Omega_{ji}^{P,S}(t) = -(\tfrac{1}{2}) f_{P,S}(t)(I_{P,S}^0)^{1/2}\langle j|\hat{\varepsilon}_{P,S}\cdot\boldsymbol{d}|i\rangle \tag{7}$$

for pump or Stokes laser field.

The explicit form of the one-photon Rabi frequency depending on the rotational quantum numbers (J', J) can be expressed for linearly polarized light as follows [16]:

$$\begin{aligned} \Omega_{\Lambda'J'M',\Lambda JM}^{P,S}(t) &= -5.335\times10^{-9}\langle\Lambda'|d(R)|\Lambda\rangle f_{P,S}(t) \\ &\quad \times(I_{P,S}^0)^{1/2}\{(2J'+1)(2J+1)\}^{1/2} \\ &\quad \times(-1)^M\begin{pmatrix} J' & 1 & J \\ -\Lambda' & \lambda & \Lambda \end{pmatrix}\begin{pmatrix} J' & 1 & J \\ -M' & 0 & M \end{pmatrix}. \end{aligned} \tag{8}$$

Here, $\langle\Lambda'|d(R)|\Lambda\rangle$ is the radial matrix element of the dipole operator $d(R)$ between the electronic states Λ' and $\Lambda(\lambda=\Lambda'-\Lambda)$. $I_{P,S}^0$ is in $\mathrm{W/cm^2}$ and all other quantities are in a.u. For $\Sigma_g^+ \leftrightarrow \Sigma_u^+$ transition, $\Lambda=\Lambda'=0$.

From Eqs. (5), the transformed Hamiltonian $[\tilde{\boldsymbol{H}}(t)]$ of the model 15-level system may be expressed as (without RWA), in the matrix form,

$$\tilde{\boldsymbol{H}}(t)=\begin{pmatrix}
0\ldots\ldots\ldots\ldots 0\ \Omega^{P}_{1,6}(1+e^{-i2\omega_{p}t})\ 0\ldots\ldots\ldots\ldots\ldots\ldots\ldots\ldots\ldots\ldots\ldots\ldots\ldots\ldots\ldots\ \ldots\ 0\\
0\ \ \Delta_{2,1}\ 0\ldots 0\ \Omega^{P}_{2,6}(1+e^{-i2\omega_{p}t})\ \Omega^{P}_{2,7}(1+e^{-i2\omega_{p}t})\ 0\ldots\ldots\ldots\ldots\ldots\ldots\ldots\ldots\ldots\ldots\ldots\ 0\\
\vdots\\
\Omega^{P}_{6,1}(1+e^{i2\omega_{p}t})\ \ \Omega^{P}_{6,2}(1+e^{i2\omega_{p}t})0\ldots 0\ \Delta^{P}_{6,1}\ \ 0\ldots 0\ \Omega^{S}_{6,11}(1+e^{i2\omega_{S}t})\ \ \Omega^{S}_{6,12}(1+e^{i2\omega_{S}t})0\ldots 0\\
\vdots\\
0\ldots\ldots 0\ \Omega^{S}_{11,6}(1+e^{-i2\omega_{S}t})\ 0\ldots\ldots\ldots\ldots\ldots\ldots\ldots 0\ \Delta^{P+S}_{11,1}\ \ 0\ldots\ldots\ldots\ldots\ldots\ldots\ldots\ldots 0\\
\vdots\\
0\ldots\ldots\ldots 0\ \Omega^{S}_{14,8}(1+e^{-i2\omega_{S}t})\ \ \Omega^{S}_{14,9}(1+e^{-i2\omega_{S}t})\ 0\ldots\ldots\ldots\ldots\ldots\ldots\ldots\ldots\ldots 0\ \Delta^{P+S}_{14,1}\,0\\
0\ldots\ldots\ldots\ldots\ldots\ldots\ldots\ldots\ldots 0\ \Omega^{S}_{15,9}(1+e^{-i2\omega_{S}t})\ \ \Omega^{S}_{15,10}(1+e^{-i2\omega_{S}t})\ 0\ldots\ldots\ldots\ldots 0\ \Delta^{P+S}_{15,1}
\end{pmatrix}. \tag{9}$$

Equations (5) have been solved for the probability amplitudes $\tilde{C}_i(t)$ $(i=1,2,\ldots,15)$ for different level populations of the model 15-level system. The populations for the initial ground, resonant intermediate, and the final target rovibrational levels evolving in time are given by $P_g(t)=|\tilde{C}_1(t)|^2$, $P_i(t)=|\tilde{C}_6(t)|^2$, and $P_f(t)=|\tilde{C}_{11}(t)|^2$, respectively. The population probability for the rest of the vibrotational levels other than the basic three rovibrational levels is $P_{rest}(t)=1-P_g(t)-P_i(t)-P_f(t)$.

It is worth mentioning here that while solving the coupled TDSE for the 15 levels, the coupling between the $v_i=1$, $J_i=1$ level of the $A\ {}^1\Sigma_u^+$ state and the rovibrational level $v_E=5$, $J_E=0$ of the higher electronic state $E\ {}^1\Sigma_g^+$, which is almost in resonance by one pump photon transition from $v_i=1$, $J_i=1$, has been neglected since it is about 2 orders of magnitude smaller than the coupling between the $v_g=0$, $J_g=0$ level of the $X\ {}^1\Sigma_g^+$ state and the $v_i=1$, $J_i=1$ level of the $A\ {}^1\Sigma_u^+$ state. It may be pointed out that with photon wavelength ~700 nm (energy ~1.77 eV), it would require three photons to reach the ionization threshold (5.145 eV) [14] of the Li_2 molecule and hence multiphoton $(1+1+1)$ ionization of Li_2 from the ground $v_g=0$, $J_g=0$ level of the $X\ {}^1\Sigma_g^+$ state via the $(1+1)$-photon resonant intermediate level $v_E=5$, $J_E=0$ of the $E\ {}^1\Sigma_g^+$ state would be improbable even for the intense but femtosecond laser pulses considered. It may also be stated that the spontaneous relaxation rate from the resonant rovibrational level $v_i=1$, $J_i=1$ of the $A\ {}^1\Sigma_u^+$ state is much smaller than the one-photon Rabi frequencies for the allowed transitions at the peak intensities and so it has not been considered in the Hamiltonian. It may be assessed that the inclusion of the irreversible processes such as multiphoton ionization, spontaneous emission, and other electronic states such as $E\ {}^1\Sigma_g^+$ in our calculations would not affect the results.

III. CALCULATIONS

We have calculated the vibrational population transfer in a model 15-level Li_2 molecular system considering five rotational levels associated with each of the initial, intermediate, and final vibrational levels (Fig. 1). The pump-laser pulse of wavelength $\lambda_P=701$ nm is taken to be in resonance with the transition from $v_g=0$, $J_g=0$ to $v_i=1$, $J_i=1$ while the Stokes laser pulse of wavelength $\lambda_S=719$ (737) nm is in resonance with the transition from $v_i=1$, $J_i=1$ to $v_f=1(2)$, $J_f=0$. The shapes, widths, and polarizations of the two pulses are assumed to be the same. For the calculation of population transfer to the final target rovibrational levels $v_f=1$ and 2, $J_f=0$ in presence of the other closely spaced rotational levels, two sets of pump and Stokes laser peak intensities are considered for each final vibrational level. For $v_f=1$, the peak intensities are $I_P^0=1.5\times10^{12}$ W/cm^2, $I_S^0=1.0\times10^{12}$ W/cm^2 and $I_P^0=1.5\times10^{13}$ W/cm^2, $I_S^0=1.0\times10^{13}$ W/cm^2. For $v_f=2$, the peak intensities are $I_P^0=1.0\times10^{12}$ W/cm^2, $I_S^0=2.5\times10^{12}$ W/cm^2 and $I_P^0=1.0\times10^{13}$ W/cm^2, $I_S^0=2.5\times10^{13}$ W/cm^2. The corresponding pulse widths are, respectively, $\tau_P(\tau_S)=50$ and 20 fs for each value of $v_f=1(2)$. For comparison, we have also computed

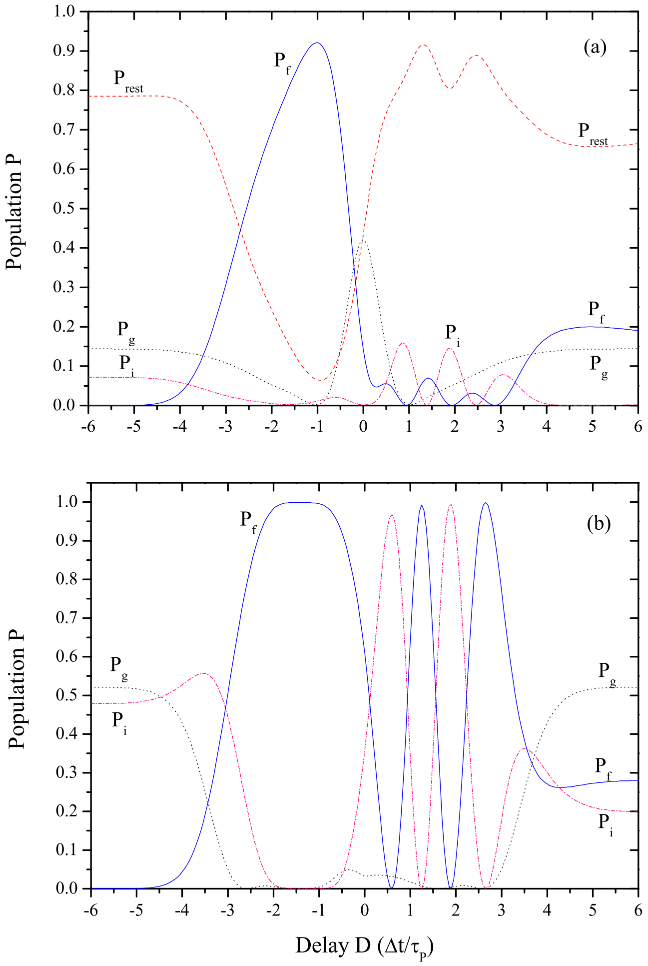

FIG. 2. (Color online) Populations (P) of different rovibrational levels of the Li$_2$ molecule plotted against (reduced) time delay (D) between the pump and Stokes laser pulses for the final-excited vibrational level $v_f=1$ ($J_f=0$) with $I_P^0=1.5\times10^{12}$ W/cm^2, $I_S^0=1.0\times10^{12}$ W/cm^2, and $\tau_P=\tau_S=50$ fs for (a) 15-level system and (b) three-level system.

the vibrational population transfer in a three-level Li$_2$ molecule with the same laser parameters.

The Born-Oppenhiemer potential energies for the $X\ {}^1\Sigma_g^+$ and $A\ {}^1\Sigma_u^+$ electronic states of the Li$_2$ molecule were obtained from the comprehensive work of Schmidt-Mink *et al.* [17] who also gave the transition electric-dipole moments. The spontaneous relaxation rate of the resonant intermediate level $v_i=1$, $J_i=1$ of the $A\ {}^1\Sigma_u^+$ state is also available from the same work. The potentials and transition dipole moments were interpolated using the cubic spline interpolation method [18].

IV. RESULTS AND DISCUSSIONS

Figure 1 depicts the schematic line diagram of the 15-level Li$_2$ molecular system with five rotational levels of the initial vibrational level $v_g=0$ of the ground $X\ {}^1\Sigma_g^+$ electronic state, five rotational levels of the intermediate vibrational level $v_i=1$ of the excited electronic state $A\ {}^1\Sigma_u^+$, and five rotational levels of the final-excited vibrational levels $v_f=1,2$ of the $X\ {}^1\Sigma_g^+$ state. The span of the five initial or final rotational levels is about 49 cm^{-1} while that of the five intermediate rotational levels is about 43 cm^{-1}. For coverage of these manifolds of rotational levels through Fourier-transform-limited bandwidth, lasers with pulse widths of not more than about 50 fs are needed.

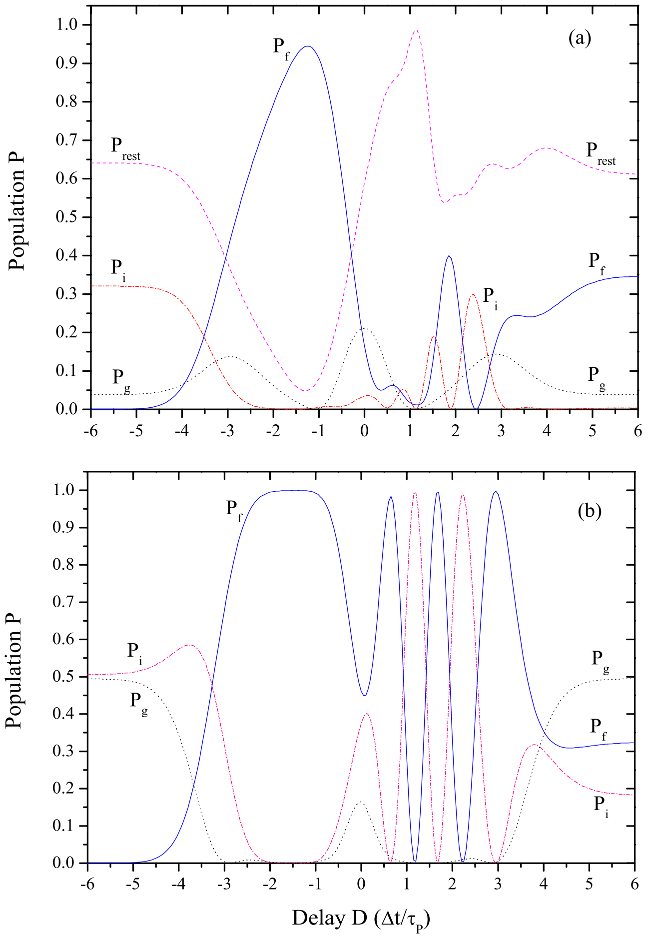

FIG. 3. (Color online) Same as in Fig. 2 except for $I_P^0=1.5\times10^{13}$ W/cm^2, $I_S^0=1.0\times10^{13}$ W/cm^2, and $\tau_P=\tau_S=20$ fs.

In Figs. 2 and 3, we have plotted the populations (P) of different rovibrational levels of the 15-level Li$_2$ alkali dimer against the reduced time delay (D) between the pulses for different pulse (peak) intensities ($I_{P,S}^0$) and pulse widths $\tau_P(\tau_S)$ of the unchirped pump and Stokes laser pulses. For comparison, we have also plotted in the figures the populations in a resonant three-level Li$_2$ molecule with the same laser parameters as for the 15-level system. The pump and Stokes peak intensities were adjusted to make the corresponding Rabi frequencies of about the same value to have the maximum population transfer [2].

Figures 2 and 3 illustrate the population transfer to the final-excited vibrational level $v_f=1$ ($J_f=0$) for $I_P^0=1.5\times10^{12}$ W/cm^2, $I_S^0=1.0\times10^{12}$ W/cm^2 with $\tau_P=\tau_S=50$ fs, and $I_P^0=1.5\times10^{13}$ W/cm^2, $I_S^0=1.0\times10^{13}$ W/cm^2 with $\tau_P=\tau_S=20$ fs, respectively. In the plots for the 15-level system [Figs. 2(a) and 3(a)], we observe that, in spite of the presence of mushrooming of rotational levels, the maximum population transfer to the final excited vibrational level $v_f=1$ (J_f

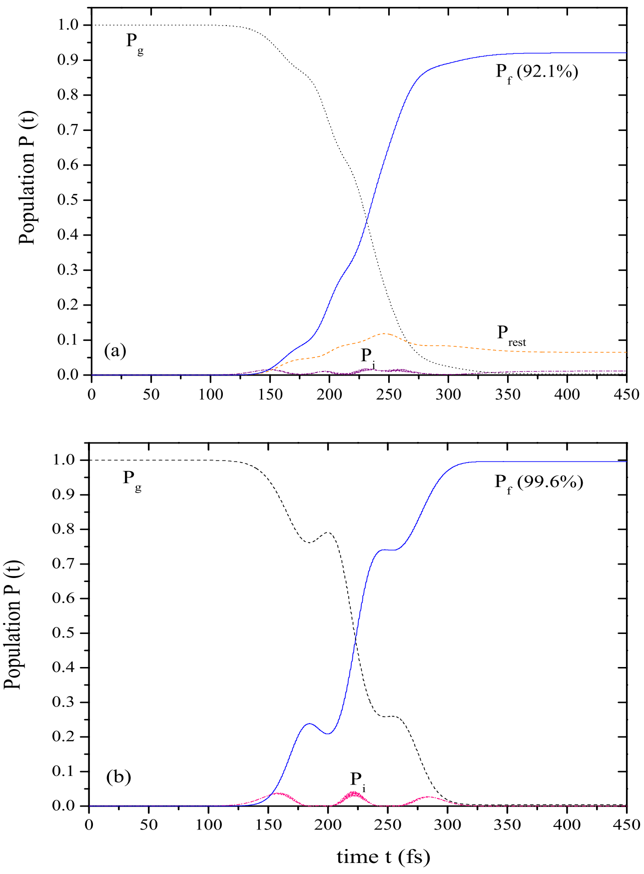

FIG. 4. (Color online) Populations $[P(t)]$ of different rovibrational levels of Li_2 molecule plotted against pulse time (t) for the final-excited vibrational level $v_f=1$ $(J_f=0)$ with $I_P^0=1.5\times10^{12}$ W/cm^2, $I_S^0=1.0\times10^{12}$ W/cm^2, and $\tau_P=\tau_S=50$ fs for counterintuitive pulse order with (reduced) pulse delay $D=-1.0$ for (a) 15-level system and (b) three-level system.

$=0)$ at the end of the pulses is about 92.1% for $I_P^0=1.5\times10^{12}$ W/cm^2, $I_S^0=1.0\times10^{12}$ W/cm^2, $\tau_P=\tau_S=50$ fs and counterintuitive pulse order with D $(\Delta t/\tau_P)=-1.0$ [Fig. 2(a)] and about 94.5% for $I_P^0=1.5\times10^{13}$ W/cm^2, $I_S^0=1.0\times10^{13}$ W/cm^2, $\tau_P=\tau_S=20$ fs with $D=-1.25$ [Fig. 3(a)], where the optimal time delay (Δt) between the pulses is near the value of pulse width τ_P (τ_S) [1]. For intuitive pulse sequence $(D>0)$, maximum population flows (at the end of the pulses) to the manifolds of the nonresonant rotational levels of the 15-level Li_2 system.

For transfer of population in a resonant three-level Li_2 system [Figs. 2(b) and 3(b)], there is a characteristic flat peak of population transfer for counterintuitive pulse order and almost complete population transfer occurs at about $-2\leq D\leq-1$. For intuitive pulse sequence, the transfer efficiency to the final target level oscillates between 0 and 1 at about $1\leq D\leq3$ [1].

In case of population transfer to the final-excited vibrational level $v_f=2$ $(J_f=0)$ for $I_P^0=1.0\times10^{12}$ W/cm^2, $I_S^0=2.5\times10^{12}$ W/cm^2 with $\tau_P(\tau_S)=50$ fs and $I_P^0=1.0\times10^{13}$ W/cm^2, $I_S^0=2.5\times10^{13}$ W/cm^2 with $\tau_P(\tau_S)=20$ fs, we have observed for the 15-level system that, even when the rotational degrees of freedom are included, efficient population transfer (>90%) to the final excited vibrational level can be achieved by unchirped femtosecond pulses. Here, the maximum population transfer to $v_f=2$ $(J_f=0)$ at the end of the pulses is about 91.2% for $I_P^0=1.0\times10^{12}$ W/cm^2, $I_S^0=2.5\times10^{12}$ W/cm^2, $\tau_P=\tau_S=50$ fs with $D=-0.75$ and about 89.8% for $I_P^0=1.0\times10^{13}$ W/cm^2, $I_S^0=2.5\times10^{13}$ W/cm^2, $\tau_P=\tau_S=20$ fs with $D=-1.1$, the optimal delay which is again near the pulse width τ_P (τ_S). For intuitive pulse order, here also maximum population is transferred (at the termination of the pulses) to the nonresonant rotational levels of the 15-level system. Hence, we can achieve efficient transfer of population to selected higher vibrational levels in the presence of mushrooming of rotational levels by controlling laser parameters.

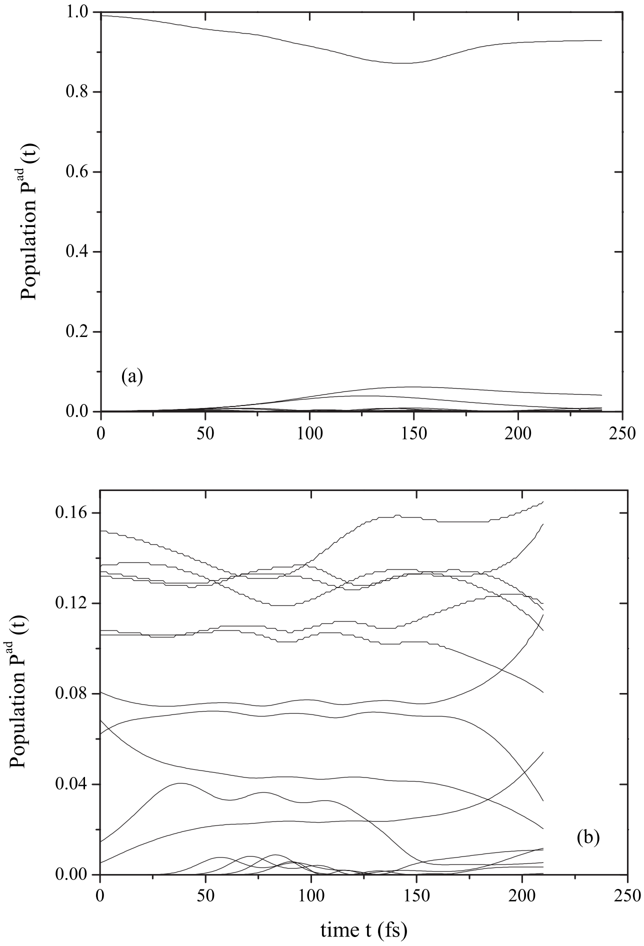

FIG. 5. Populations $[P^{ad}(t)]$ of the 15-level Li_2 molecule plotted against pulse time (t) in the adiabatic picture for the final-excited vibrational level $v_f=1$ $(J_f=0)$ with $I_P^0=1.5\times10^{12}$ W/cm^2, $I_S^0=1.0\times10^{12}$ W/cm^2, and $\tau_P=\tau_S=50$ fs for (a) counterintuitive pulse sequence with (reduced) time delay $D=-1.0$ and (b) intuitive pulse sequence with $D=1.0$.

Figure 4 shows the populations $P(t)$ of different rovibrational levels as a function of pulse time (t) for $I_P^0=1.5\times10^{12}$ W/cm^2, $I_S^0=1.0\times10^{12}$ W/cm^2, and $\tau_P=\tau_S=50$ fs with target vibrational level $v_f=1$ $(J_f=0)$ for the 15- and three-level Li_2 systems. The pulse order is counterintuitive with (reduced) pulse delay $D=-1.0$. From the plots, we see that for the 15-level molecular system [Fig. 4(a)], there is very small population transfer (P_i) to the intermediate resonant level throughout the pulse duration and at the end of the pulses, about 92.1% population is transferred to the final $v_f=1$ ($J_f=0$) level while only about 6.5% population transfer (P_{rest}) takes place to the rest of the nonresonant rotational levels. For the three-level molecule [Fig. 4(b)], there is some transient population transfer (P_i) to the resonant intermediate level and about 99.6% population (P_f) is transferred to the final $v_f=1$ ($J_f=0$) level at the termination of the pulses [19].

In case of population transfer $P(t)$ to $v_f=2$ ($J_f=0$) for $I_P^0=1.0\times10^{12}$ W/cm^2, $I_S^0=2.5\times10^{12}$ W/cm^2, and $\tau_P=\tau_S=50$ fs, we have observed, for the 15-level system, that there is negligible transient population transfer (P_i) to the resonant intermediate level during the pulse period and about 88.7% population transfer (P_f) takes place to the final target level $v_f=2$ ($J_f=0$) at the end of the pulses while about 1% population (P_{rest}) flows to the rest of the nonresonant rotational levels. So, we can have selective and efficient transfer of population to target higher vibrational levels in the presence of manifolds of rotational levels by choosing proper laser parameters.

The population transfer in the 15-level Li_2 molecular system can be explained by plotting the populations with time in the adiabatic picture [20]. In Fig. 5, we have depicted the adiabatic populations $P^{ad}(t)$ as a function of time t for the 15-level system taking $I_P^0=1.5\times10^{12}$ W/cm^2, $I_S^0=1.0\times10^{12}$ W/cm^2, and $\tau_P=\tau_S=50$ fs for $v_f=1$ ($J_f=0$). In presenting the figure, we have, for clarity, not considered the highly oscillatory counter-rotating wave terms. Figure 5(a) shows $P^{ad}(t)$ for counterintuitive pulse order with (reduced) time delay $D=-1.0$ while Fig. 5(b) shows $P^{ad}(t)$ for intuitive pulse sequence with $D=1.0$. It is seen that, for $D=-1.0$, there is almost an adiabatic passage resulting in an *efficient* and *selective* population transfer to the final-excited vibrational level $v_f=1$ ($J_f=0$) at the end of the pulses [cf. Fig. 4(a)]. Figure 5(a) does not show complete population inversion, since there is some population in the other levels. The final adiabatic transfer of the population depends on a number of laser parameters, such as intensities, pulse widths, pulse delay, etc. The population inversion can be improved to some extent by making the Rabi frequencies larger. For example, doubling the intensities, keeping the other laser parameters constant, results in a slightly larger inversion (∼95%). Figure 5(b) shows that for $D=1.0$, there is no adiabatic passage resulting in negligible population transfer to the target vibrational level. The total population from the initial ground level flows to all the other relevant rotational levels of the system due to nonadiabatic coupling between these states [4] [cf. Figs. 2(a) and 3(a)].

V. CONCLUSION

We have theoretically studied the vibrational population transfer in the presence of mushrooming of rotational levels in a model multilevel Li_2 alkali dimer by STIRAP process. We have observed that the mushrooming of rotational levels significantly changes the dynamics of population transfer by ultrashort intense laser pulses since the rotational levels do not respond adiabatically due to nonadiabatic coupling between them. Nevertheless, the effect of mushrooming of rotational levels can be controlled to achieve efficient and selective population transfer to excited target vibrational levels for counterintuitive pulse sequence with intense unchirped femtosecond pump and Stokes laser pulses. We have attempted to explain the population transfer in the adiabatic picture.

[1] K. Bergmann, H. Theuer, and B. W. Shore, Rev. Mod. Phys. **70**, 1003 (1998).

[2] N. V. Vitanov, T. Halfmann, B. W. Shore, and K. Bergmann, Annu. Rev. Phys. Chem. **52**, 763 (2001), and references cited therein.

[3] U. Gaubatz, P. Rudecki, M. Becker, S. Schiemann, M. Külz, and K. Bergmann, Chem. Phys. Lett. **149**, 463 (1988).

[4] U. Gaubatz, P. Rudecki, S. Schiemann, and K. Bergmann, J. Chem. Phys. **92**, 5363 (1990).

[5] Y. B. Band and P. S. Julienne, J. Chem. Phys. **94**, 5291 (1991).

[6] B. W. Shore, K. Bergmann, J. Oreg, and S. Rosenwaks, Phys. Rev. A **44**, 7442 (1991).

[7] G. W. Coulston and K. Bergmann, J. Chem. Phys. **96**, 3467 (1992).

[8] N. V. Vitanov and S. Stenholm, Opt. Commun. **127**, 215 (1996); **135**, 394 (1997); Phys. Rev. A **55**, 648 (1997); **55**, 2982 (1997); **56**, 741 (1997); **56**, 1463 (1997).

[9] N. V. Vitanov and S. Stenholm, Phys. Rev. A **60**, 3820 (1999).

[10] S. Ghosh, S. Sen, S. S. Bhattacharyya, and S. Saha, Phys. Rev. A **59**, 4475 (1999).

[11] S. Ghosh, S. Sen, S. S. Bhattacharyya, and S. Saha, Pramana, J. Phys. **54**, 827 (2000).

[12] F. Légaré, S. Chelkowski, and A. D. Bandrauk, J. Raman Spectrosc. **31**, 15 (2000).

[13] Y. B. Band, S. Kallush, and R. Baer, Chem. Phys. Lett. **392**, 23 (2004).

[14] A. A. Radzig and B. M. Smirnov, *Reference Data on Atoms, Molecules and Ions*, Chemical Physics Vol. 31 (Springer, New York, 1985).

[15] B. W. Shore, *The Theory of Coherent Atomic Excitation* (Wiley, New York, 1990), Vol. 1, Chap. 3, Sec. 9.

[16] S. Sen, S. Ghosh, S. S. Bhattacharyya, and S. Saha, J. Chem. Phys. **116**, 1286 (2002).

[17] I. Schmidt-Mink, W. Müller, and W. Meyer, Chem. Phys. **92**, 263 (1985).

[18] N. E. Greville, in *Mathematical Methods for Digital Computers*, edited by A. Ralston and H. S. Wilf (Wiley, New York, 1967), Vol. 2, p. 156.

[19] C. C. Shu, J. Yu, K. J. Yuan, W. H. Hu, J. Yang, and S. L. Cong, Phys. Rev. A **79**, 023418 (2009).

[20] K. J. Yuan, Z. G. Sun, S. L. Cong, S. M. Wang, J. Yue, and N. Q. Lou, Chem. Phys. **316**, 245 (2005).